

ABUNDANCE ESTIMATES FOR THE DISTANT ANTICENTER CLUSTERS KING 8 AND Be 19

C. A. CHRISTIAN¹

Canada-France-Hawaii Telescope Corp./University of Hawaii

Received 1984 January 30; accepted 1984 May 3

ABSTRACT

Intensified Image Dissector Scanner data were used to analyze the spectra of suspected members of the distant anticenter clusters King 8 and Be 19. The results are: (1) two early-type cluster members were identified in King 8. Their spectral types, $\leq A5$, are consistent with the stars' photometric positions in the cluster color-magnitude diagram (near main-sequence turnoff), providing a verification of the photometrically derived age of the cluster. (2) Several foreground stars also were identified in both fields through the use of simulated photometric indices. (3) Spectrophotometric data for suspected cluster giants suggest that both clusters may be slightly metal-poor, i.e., with abundances similar to NGC 2158 and NGC 2420 ($[Fe/H] = -0.5$). (4) Assuming that all three clusters, King 8, Be 19, and NGC 2158, have abundances $[Fe/H] = -0.4 \pm 0.1$, the galactic abundance gradient is $d[Fe/H]/dR = -0.08 \text{ dex kpc}^{-1}$ for objects older than $5 \times 10^8 \text{ yr}$, in agreement with previous studies.

Subject headings: clusters: open — galaxies: Milky Way — galaxies: stellar content — spectrophotometry — stars: abundances

I. INTRODUCTION

Abundance studies in star clusters can provide elemental information about galactic evolution. For example, surveys of globular clusters have provided difficult constraints for theoreticians (cf. reviews by Freeman 1980; Kraft 1979; Zinn 1983, and references therein). Investigations of the diverse clusters found in Local Group galaxies have spawned theories interrelating abundances, luminosity functions, and stellar populations with parent galaxy morphology and local environment.

Detailed investigations of open clusters in the Galaxy frequently have concentrated upon the nearest, brightest, or most spectacular clusters which are the easiest to study. Observational difficulties arise because many disk clusters are sparsely populated and have ill-defined memberships. The situation for more distant objects is aggravated by field star contamination and reddening effects.

Nonetheless, distant open clusters represent practical tools for probing the galactic disk, particularly in the anticenter where the outermost parts of the galactic plane can be surveyed. Numerous small, remnant clusters have been found in the anticenter; remarkably, these objects have survived the dynamical forces imposed upon them. Many of these clusters, with intermediate ages ($0.5\text{--}5.0 \times 10^9 \text{ yr}$), remain as witnesses to a poorly understood epoch in the history of the galactic disk. If similar objects were able to form in the solar neighborhood, they unfortunately would have evaporated long ago, leaving their members scattered over large regions in the disk (cf. Janes and Adler 1982). In this work, observations of two distant intermediate-age anticenter clusters, King 8 and Be 19, were used to estimate the cluster abundances. In § II the spectrophotometry and construction of metallicity-sensitive indices are presented; § III contains results for the stars surveyed. A discussion of this study in the context of investigations of the galactic disk is contained in § IV.

II. OBSERVATIONAL MATERIAL AND MEASUREMENTS

a) Background

The two clusters chosen for the spectrophotometric study, Be 19 (C0521+295) and King 8 (C0546+336), had been surveyed previously with broad-band photometry (Christian 1980 [Paper I]; 1981 [Paper II]). This photometric work suggested that the poorly populated cluster Be 19 is $\sim 3 \times 10^9 \text{ yr}$ old, with an intrinsic distance modulus equal to $13.5 \pm 0.5 \text{ mag}$ and reddening $E(B-V) = 0.4 \pm 0.1 \text{ mag}$. King 8 is believed to be younger, i.e., $\sim 8 \times 10^8 \text{ yr}$, at $(m-M)_0 = 13.7 \pm 0.3 \text{ mag}$ and $E(B-V) = 0.7 \pm 0.1 \text{ mag}$. These two clusters have galactocentric distances greater than $3 \text{ kpc} + R_0$,² as they are situated in the direction of the galactic anticenter.

b) Candidate Selection

Candidate members were chosen initially with reference to the cluster color-magnitude diagrams (C-M diagrams). In distant clusters, foreground contamination is severe, but as shown in Paper II and by Christian (1982), reddening effects actually can be an asset in constructing membership criteria. That is, an estimate of the cluster reddening can be coupled with slitless spectroscopic observations to sift out cluster members from the sea of contaminating field stars. Fortunately, the selection of stars in the field of King 8 could be further refined using this technique. In each cluster a few stars near the main-sequence turnoff were selected to verify the cluster ages presented in Papers I and II. The majority of the program objects were redder stars, suspected to be cluster giants.

c) Spectrophotometry and Photometric Indices

Intermediate-band spectrophotometry, at 9.5 \AA resolution, was obtained with the Intensified Image Dissector Scanner (IIDS) on the Kitt Peak National Observatory (KPNO) 2.1 m telescope and reduced at KPNO according to the procedures

¹ Visiting astronomer, Kitt Peak National Observatory operated by AURA, Inc., under contract with the National Science Foundation.

² R_0 = Galactocentric distance of the Sun.

described in Paper II. The data, accumulated during three observing sessions (1979–1981), were acquired using grating number 26 (600 lines mm^{-1}) centered at 4500 Å (1979) or 4700 Å (1980, 1981) and a 4" aperture. Sample scans appear in Figure 1. The analysis of the spectrophotometric data involved examination of empirical relationships among simulated spectrophotometric indices with an eye to similar studies of both disk and halo objects (cf. Spinrad and Taylor 1969; Fay, Stein, and Warren 1973; Roman 1973; van den Berg and Pritchett

1977, to mention a few). Consideration of classical classification criteria (Morgan, Keenan, and Kellman 1942; Keenan and McNeil 1976) and visual examination of the observed spectrophotometric scans led to the definition of the array of spectral indices listed in Table 1. The behavior of these indices as a function of spectral class was reviewed using the grid of comparison stars observed with the IIDS during the three observing runs mentioned above. This grid of stars, numbering over 100, includes field stars, IIDS standards (Strom 1977), and

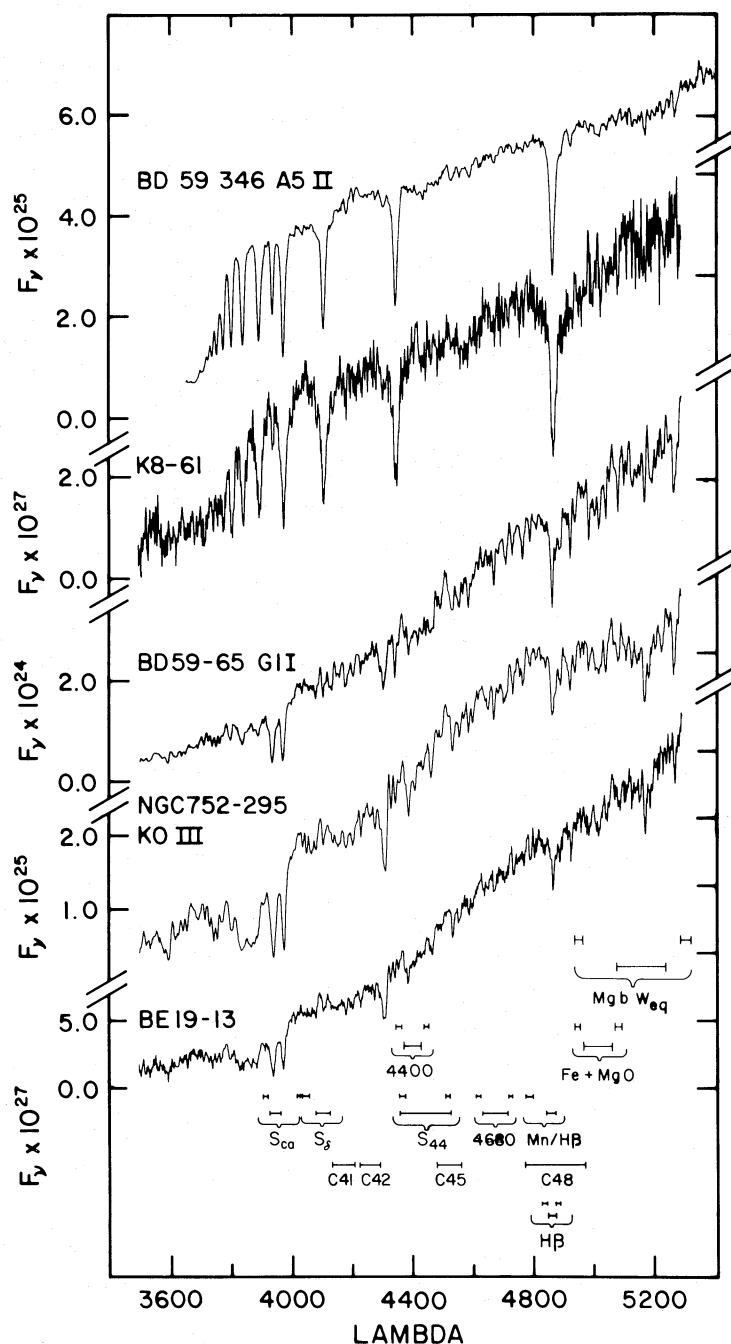


FIG. 1.—Sample IIDS scans. Units of flux are $\text{ergs cm}^{-2} \text{s}^{-1} \text{\AA}^{-1}$. The star BD +59°346 is shown in comparison to King 8-61 which is suspected to be a cluster member. Examination of the two spectra indicates that No. 61 is a main sequence or turnoff star in King 8. Typical features include broader hydrogen lines and weak atomic blends in King 8-61. The star Be 19-13 is suspected to be a cluster giant. Other stars are shown to indicate luminosity and temperature effects (BD +65°59 and NGC 752-295). At the bottom of the figure are shown the approximate bandpasses for the simulated photometric indices.

TABLE 1
 SIMULATED PHOTOMETRIC INDICES

Index	γ_c (Å)	$\Delta\lambda$ (Å)	Feature, Reference
C(45–48)	4515	84	DDO color, McClure and van den Bergh 1968
	4888	176	
C(42–45)	4255	82	DDO color, McClure and van den Bergh 1968
	4513	84	
C(41–42)	4165.0	84	DDO color (CN), McClure and van den Bergh 1968
	4255.0	84	
H β	4838.8	19	H β equivalent width, Burstein <i>et al.</i> 1982 Calibrated for late-type stars
	4885.0	14	
	4863.3	28	
W_{eq} (4680)	4621.0	20	Atomic blend λ 4780, this paper
	4730.0	20	
	4680.0	80	
W_{eq} (4400)	4360.0	20	Atomic blend λ 4400, this paper
	4450.0	20	
	4405.0	50	
S_{44}	4360.0	17	Atomic blend λ 4400, Christian and Smith 1983
	4509.0	18	
	4436.0	148	
Mn/H β	4788.0	22	Atomic blend λ 4780 vs. H β , this paper
	4861.0	28	
S_δ	4051.0	23	H δ index, Christian and Smith 1983
	4103.0	39	
S_{Ca}	3910.0	12	Ca H, K index, Christian and Smith 1983, calibrated for early-type stars
	4022.0	12	
	3934.0	40	
Fe + MgO	4950.0	20.0	Blend at λ 5005, this paper
	5070.0	20.0	
	5005.0	90.0	
Mg b W_{eq}	4950.0	20.0	Equivalent width of Mg b feature, this paper
	5300.0	20.0	
	5170.0	120.0	

cluster members. The latter stars were particularly useful for estimating the metallicities represented in the program objects, as the selected clusters have independently measured ages and abundances. The sensitivity of the constructed indices to stellar parameters was rechecked using the library of stellar spectra obtained by Jacoby, Hunter, and Christian (1984) with the KPNO 90 cm Intensified Reticon Scanner (IRS). These data are intended specifically to supplement projects completed with the IIDS by providing similar spectrophotometry of stars which completely span the H-R diagram.

Many of the indices listed in Table 1 were based upon photometric systems described in the literature, in order to relate the IIDS (or IRS) data to previous cluster work. The spectrophotometry was calibrated by comparing the calculated indices directly to published values. An additional set of nearly “reddening-free” indices was computed because many of the published photometric indices are subject to reddening effects, giving ambiguous results for objects suffering from large but ill-determined amounts of interstellar extinction. Problems related to uncertain reddening values can arise even in the investigation of objects with relatively low reddening values; see, for example, the discussion of the abundance of NGC 2477 by Smith and Hesser (1983).

Deliberation on a variety of combinations of the indices led to the selection of a few “two-index” diagrams that best represent the variations seen in the spectrophotometry. Sample IIDS scans appear in Figure 1, along with a schematic representation of the indices used.

III. BEHAVIOR OF SPECTRAL INDICES AND RESULTS FOR PROGRAM STARS

In this section, the spectral indices simulated from the IIDS data are examined. The values for program objects were compared to the grid of field and cluster stars. The clusters NGC 752, NGC 1245, NGC 2158, and NGC 2420 were chosen as comparison objects because their ages and abundances span the ranges appropriate for the two program clusters. Some members of these comparison clusters, measured at a variety of spectral resolutions, have reasonably well determined intrinsic stellar parameters. Globular cluster stars in M3 and M15 were included to investigate the behavior of severely metal-poor stars, due to the lack of very metal deficient intermediate-age disk clusters. Given the level of photometric precision in the simulated indices and the fact that the influence of age upon the spectral indices is swamped by abundance effects for this sample, the disparity in age between the various clusters did not appear to be a detrimental factor in the analysis.

a) DDO Photometric Indices

DDO photometry has been used in a variety of applications, including abundance studies of disk G and K stars to investigate metallicity gradients in the galactic plane (Janes 1979a and references therein) and in studies of globular cluster abundances, as in the studies by Hesser, Hartwick, and McClure 1977 (HHM). Unfortunately, DDO indices are highly sensitive to reddening effects. Therefore, in this investigation, DDO

TABLE 2
PHOTOMETRIC INDICES CALCULATED FROM SPECTRA OF IIDS CALIBRATION GRID

Object	C(45-48)	C(42-45)	C(41-42)	H β	(4680)	(4400)	S ₄₄	Mn/H β	S δ	S _{Ca}	Fe+MgO	Mgb W _{eq}
M15												
I-38	1.185	0.651	0.093	1.157	0.337	1.363	4.167	0.359	0.58	1.24	0.177	-0.748
P8 ^a	1.114	0.577	0.057	1.392	1.199	0.847	4.192	0.150	0.60		-0.464	-3.733
S1	1.288	0.784	0.127	1.071	-0.403	0.295	4.159	0.208	0.57	1.11	0.454	0.244
S4	1.340	0.863	0.142	1.157	1.182	1.041	4.103	0.192	0.55		0.748	-0.394
S6	1.284	0.791	0.126	0.730	1.152	1.604	4.103	0.384	0.55	1.02	1.012	0.952
S36	1.168	0.615	0.095	1.193	0.714	0.423	4.168	0.210	0.59	1.31	0.081	-1.939
II-54 ^a	1.234	0.662	0.109	1.182	1.169	-0.551	4.250	0.129	0.66		0.040	-0.998
M3												
I-II-18	1.182	0.663	0.091	1.142	2.208	-1.781	4.189	0.136	0.56	0.96	2.949	
I-III-28	1.320	0.906	0.152	0.961	1.515	0.814	3.979	0.157	0.54	0.83	1.943	
X23	1.273	0.914	0.135	1.388	2.173	0.691	4.004	0.228	0.54	0.75	2.819	
193	1.131	0.737	0.046	1.590	2.356	0.210	4.203	0.228	0.57	1.12	1.186	
216	1.181	0.731	0.080	1.469	1.472	0.423	4.094	0.210	0.54	0.92	2.539	
237 ^a	1.042	0.622	0.001	3.529	2.844	1.770	4.052	0.021	0.57	1.06	1.066	
NGC752												
77	1.179	0.856	0.176	1.607	4.617	4.747		0.084	0.53	0.82	3.344	
108	0.900	0.408	0.046	5.011	0.978	-0.763	4.185	-0.096	0.70	1.27	1.370	
110	1.113	0.714	0.133	2.645	3.616	2.967	4.000	0.039	0.61	1.08	2.617	
117	0.932	0.446	0.055	4.903	0.872	-1.093	4.219	-0.095	0.71	1.31	1.732	
123	0.877	0.501	0.050	5.517	1.531	-1.785	4.273	-0.038	0.72	1.31	1.486	
135	0.924	0.455	0.055	5.113	0.828	-1.240	4.254	-0.940	0.69	1.25	1.025	
166	0.874	0.574	0.043	5.424	0.377	-1.209	4.253	-0.066	0.73	1.31	1.358	
208	1.134	0.922	0.132	1.825	7.446	5.737	3.863	0.070	0.52	0.84	2.904	
222	0.879	0.505	0.029	5.218	0.732	-1.848	4.222	-0.036	0.77	1.36	1.020	
295	1.147	0.812	0.132	1.852	3.371	4.247	3.924	0.080	0.55	0.84	2.927	
NGC1245												
5 ^a	1.109	0.893	0.017	1.393	3.933	5.692	3.884	0.091	0.49	0.89	2.863	
12	0.942	0.433	0.073	6.976	0.542	-2.242	4.355	-0.248	0.84	1.40	2.702	
70	1.187	0.799	0.137	1.749	2.664	2.949	4.167	0.167	0.57	0.92	0.187	
NGC2158												
c	1.019	0.531	0.049	4.248	-0.103	-1.211	4.268	-0.020	0.69	1.30	2.048	2.646
I-5-28	1.168	1.065	0.119	1.617	7.552	7.096	3.754	0.141	0.52	0.79	-0.037	26.767
3-4-1	1.399	1.039	0.218	1.355	4.344	6.164	3.788	0.182	0.50	0.61	3.461	11.674
4-2-69	1.475	1.359	0.261	0.629	5.293	6.292	3.632	0.248	0.50	0.42	5.697	23.041
4-4-13	1.264	0.922	0.138	0.981	2.896	4.842	3.831	0.162	0.54	0.64	4.177	6.627
NGC2420												
A	1.283	0.966	0.271	1.124	4.190	5.762	3.821	0.165	0.52	0.64	5.017	18.918
D	1.165	0.746	0.155	1.871	3.583	2.729	3.968	0.091	0.56	0.95	3.490	10.945
F	1.228	0.878	0.213	1.668	4.239	4.239	3.866	0.128	0.55	0.90	4.191	16.263
Q	1.183	0.807	0.175	1.438	3.272	3.714	3.905	0.127	0.53	0.87	4.652	14.052
X ^b	1.446	0.993	0.674	1.223	12.296	4.341	4.155	0.116	0.62	1.00	1.686	22.429
II-3-44	1.170	0.792	0.137	1.778	2.683	3.058	3.919	0.115	0.54	0.94	3.298	13.259
Lick Standards^c												
HR1805	1.392	1.218	0.383	0.837	8.105	7.709	3.709	0.334	0.53	0.51	5.091	25.718
HR2002	1.211	0.870	0.246	2.071	6.236	5.067	3.852	0.113	0.56	0.79	4.996	12.615
HR2600	1.317	1.047	0.202	1.702	3.048	4.588	3.795	0.197	0.54	0.54	4.030	15.190
HD2665	1.146	0.646	0.032	1.803	0.479	0.753	4.240	0.148	0.60	1.21	0.630	0.228
HD88609	1.165	0.633	0.080	0.853	1.030	1.030	4.175	0.351	0.59	1.33	1.053	0.824
Late type field stars												
BD+15 2380	1.177	0.811	0.097	1.242	2.600	3.230	3.981	0.106	0.56	0.81	2.925	
BD+22 1187	1.288	0.881	0.154	1.924	-0.054	2.193	3.963	0.107	0.61	0.93	1.314	
BD+38 2283	1.104	0.889	0.016	1.292	3.907	4.849	3.869	0.084	0.51	0.87	2.384	
BD+54 1323	1.092	0.555	0.016	2.138	1.079	0.536	4.143	0.106	0.60	1.25	-0.108	
BD+56 84	1.226	0.683	0.094	3.952	1.690	2.643	3.814	0.084	0.59	0.72	5.246	12.303
BD+59 65	1.216	0.792	0.126	3.123	1.962	2.748	3.797	0.103	0.57	0.92	5.422	
HD 13884	1.221	1.105	0.241	0.595	7.542	7.791	3.774	0.141	0.52	0.52	4.427	
HD 105446	1.094	0.571	0.024	1.635	1.043	-0.359	4.170	0.104	0.59	1.11	1.515	
HD 108077	1.178	0.870	0.092	1.730	4.234	3.237	4.001	0.083	0.55	0.82	3.561	
COMA 132	1.059	0.696	-0.008	2.679	3.526	2.190	4.000	0.035	0.56	0.56	1.602	

^a Suspected nonmember (Sandage 1970; Trefzger *et al.* 1983).

^b Ba star (McClure *et al.* 1974).

^c Burstein *et al.* 1983; Suntzeff 1980.

TABLE 3
SPECTRAL TYPE ESTIMATES AND PHOTOMETRIC PROPERTIES OF PROGRAM STARS

Object	Sp. ^a	<i>V</i> ^b	<i>B</i> - <i>V</i> ^b	<i>C</i> (45-48)	<i>C</i> (42-45)	<i>C</i> (41-42)	<i>E</i> (<i>B</i> - <i>V</i>) ^c	Spectral ^e Type	[Fe/H] ^c	Comment, References
King 8:										
7	G6 II-III	15.46	1.29	1.282	0.905	0.158	0.4	G8 II-III	-0.3	Model 5000/1.5 + 0.0 to -0.5 (1)
33	⟨F0 V	16.25	0.56	1.074	0.483	0.082	>0.35	⟨F8		Main sequence turnoff star
35	~G III	16.07	1.30	1.242:	0.821:	0.109:	0.6	G5 IV	-0.3	HD 14174 (2)
61	⟨F0 V	16.52	0.64	1.080	0.514	0.116	≥0.35	⟨F8		Main sequence turnoff star
105 ^e	F5, field	13.61	0.19	1.077	0.573	0.091	~0.0	⟨F8		Field star
107	G8 III	15.70	1.25	1.348	0.823	0.185	0.5	G4 II-III	-0.3	<i>B</i> - <i>V</i> slightly blue for DDO colors
109	field G V	15.50	1.10	1.079	0.700	0.035	0.0-0.1	G3 V	0.0?	<i>B</i> - <i>V</i> very red for DDO colors
119	G III	16.20	1.12	1.219	0.841	0.057	0.1-0.2	G9 III-II	-0.5	Low S/N spectrum
143	G7 II-III	15.80	1.45	1.349	0.926	0.256	0.5	G8 II	-0.5	Model 4500-5000/2.25/-0.5 (1)
Be 19:										
3	G-K V	16.36	1.24	1.218	1.030	0.080	0.1	K3 IV-V	0.0	
13	~K0 III	14.68	1.27	1.256	0.903	0.160	0.2-0.3	K0 III-IV	-0.2	
30	G6 III	16.36	1.24	1.236	0.766	0.202	0.35	G4 III-II	-0.2	Low S/N spectrum
33	G5 III	16.26	1.22	1.251	0.858	0.130	0.30	G8 III	-0.3	
75	Field K5 V	16.22	1.33	1.200	1.226	0.023	0.0	K5 V	0.0	
83	G3 III	16.17	1.22	1.281	0.759	0.109	0.4	G0 II?	-0.3	Low S/N spectrum
101	G2 III	16.97	1.24	1.193	0.799	0.075	0.3	G2 III-II	-0.3	
106	Poor S/N	17.93	0.89	1.192	0.524	0.041	~0.3	⟨F8		
116	G2 III	16.78	1.24	1.232	0.798	0.124	0.3	G2 III-II	-0.3	

^a Spectral types from visual examination of IIDS spectrophotometry, ± 3 spectral type subdivisions.

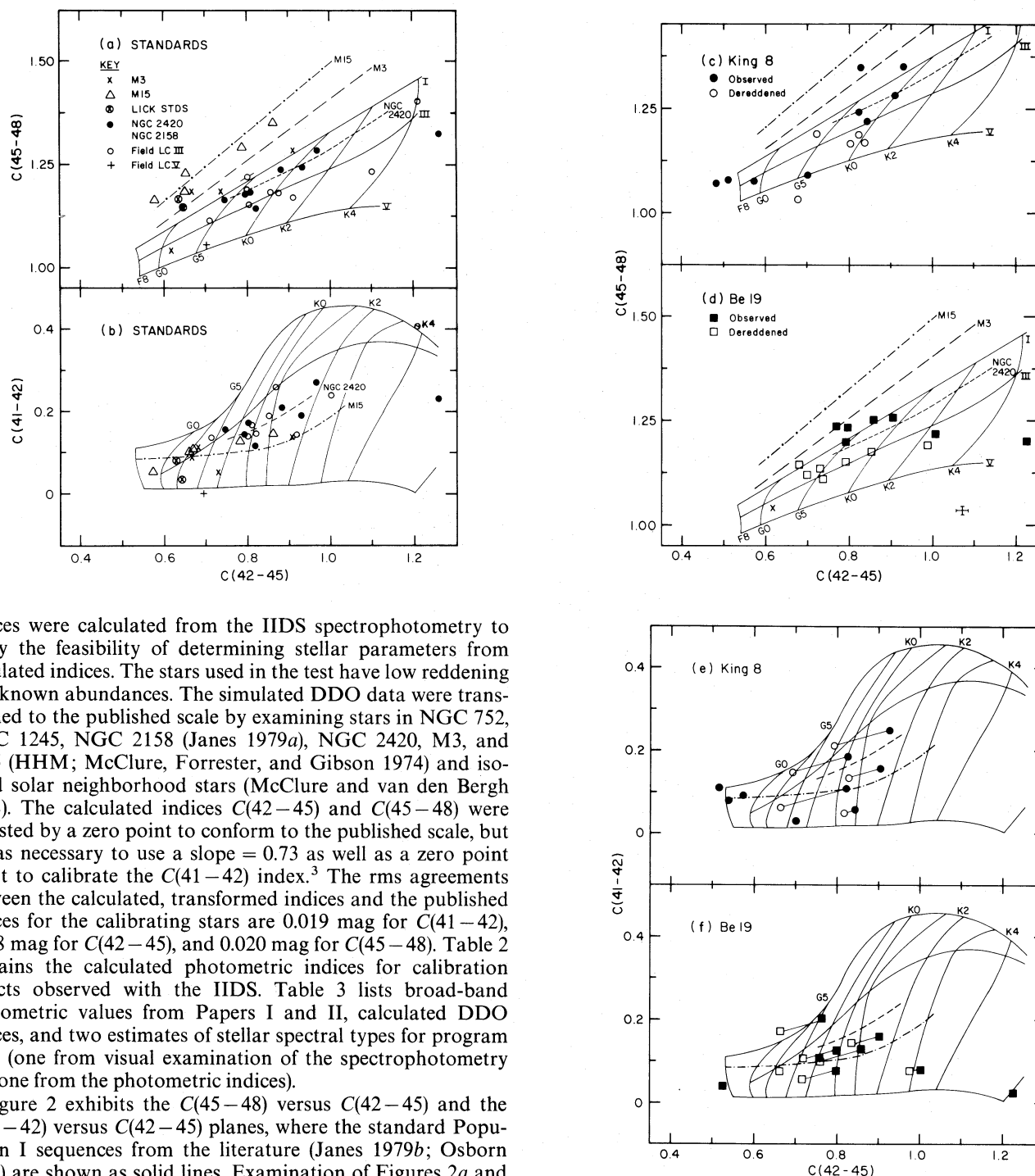
^b Taken from Paper I (King 8) and Paper II (Be 19).

^c Values most consistent with *B*, *V*, and DDO photometry. Spectral types nomenclature taken from Osborn's (1979) calibration of *B* - *V*, *C*(45-48), and *C*(42-45), not corrected for *C*(41-42) or abundance estimates.

^d Values less certain due to possible contamination in sky aperture.

^e Probably nonmember (Paper I).

REFERENCES:—(1) Bell and Gustafsson 1978. (2) Hartkopf and Yoss 1983.



indices were calculated from the IIDS spectrophotometry to study the feasibility of determining stellar parameters from simulated indices. The stars used in the test have low reddening and known abundances. The simulated DDO data were transformed to the published scale by examining stars in NGC 752, NGC 1245, NGC 2158 (Janes 1979a), NGC 2420, M3, and M15 (HHM; McClure, Forrester, and Gibson 1974) and isolated solar neighborhood stars (McClure and van den Bergh 1968). The calculated indices $C(42-45)$ and $C(45-48)$ were adjusted by a zero point to conform to the published scale, but it was necessary to use a slope = 0.73 as well as a zero point offset to calibrate the $C(41-42)$ index.³ The rms agreements between the calculated, transformed indices and the published indices for the calibrating stars are 0.019 mag for $C(41-42)$, 0.018 mag for $C(42-45)$, and 0.020 mag for $C(45-48)$. Table 2 contains the calculated photometric indices for calibration objects observed with the IIDS. Table 3 lists broad-band photometric values from Papers I and II, calculated DDO indices, and two estimates of stellar spectral types for program stars (one from visual examination of the spectrophotometry and one from the photometric indices).

Figure 2 exhibits the $C(45-48)$ versus $C(42-45)$ and the $C(41-42)$ versus $C(42-45)$ planes, where the standard Population I sequences from the literature (Janes 1979b; Osborn 1979) are shown as solid lines. Examination of Figures 2a and 2b shows that the calculated data for giants in NGC 752, NGC 1245, and solar neighborhood stars (all called "field") fall near the published solar abundance sequences, as expected. Second, the calculated DDO indices for stars in M15 and M3 which do not have previously published DDO photometry (shown as triangles and crosses) scatter close to the sequences defined by

³ The computed $C(41-42)$ index apparently suffers from the fluxing procedure previously used at KPNO to calibrate IIDS data (cf. Suntzeff 1980 and Paper II). Fortunately, the measurement of a good number of calibration stars (i.e., those with published photometry) ensured that the "fluxed" data could be rectified to the published scale.

FIG. 2.—The $C(45-48)$ vs. $C(42-45)$ and $C(41-42)$ planes for (a, b) calibration objects, (c, e) King 8, and (d, f) Be 19. The loci of Population I stars from Osborn (1979) are shown as solid lines; sequences for the clusters M3 ($[Fe/H] = -1.4$), M15 ($[Fe/H] = -2.2$), and NGC 2420 ($[Fe/H] = -0.5$), derived from published photometry also are labeled. In (a) and (b), values calculated only for M3 and M15 stars that do not have previously measured DDO indices are shown in addition to data for field stars, NGC 2420 and NGC 2158. In (c-f), the two circled crosses represent HD 2665 and HD 88609, two extremely metal-poor stars used as standards by Suntzeff (1980). The data for King 8 are shown as circles: those for Be 19 are squares. Filled symbols represent observed values; unfilled symbols indicate a reddening correction has been applied, commensurate with the iterative procedure described in the text. The figures demonstrate the greater scatter in the simulated indices as well as the need for reddening-free measurements.

the published photoelectric photometry (*dot-dashed line* and *long dashed line*, respectively). The most discrepant point in the M15 data is that for star P8. This star is not a firmly verified member (Trefzger *et al.* 1983) and therefore should not be expected to follow the M15 data. The membership criteria for M3 are scant; but, again, the most discrepant star, 237, has long been considered a nonmember (Sandage 1970). The data representing HD 2665 and HD 88609, two extremely metal-poor standards (Suntzeff 1980), shown as encircled crosses in Figures 2*a* and 2*b*, also fall in the expected location, near the globular cluster stars. These two stars as well as M3 and M15 were included in the observing program as examples of extremely metal deficient stars ($[\text{Fe}/\text{H}]_{\text{M3}} \sim -1.4$ and $[\text{Fe}/\text{H}]_{\text{M15}} < -2.0$; HHM) due to the lack of known low-metallicity, intermediate-age clusters. The precise values of $[\text{Fe}/\text{H}]$ for the extremely metal-poor stars are not an issue in this study because the program stars do not appear to be more metal-poor than $[\text{Fe}/\text{H}] = -1.0$ (see below).

Finally, consider the short dashed line in the figures, which represents published and calculated data for NGC 2420 stars. The sparse IIDS data for NGC 2158 giants, i.e., stars 3-4-1, 4-2-69, and 4-4-13 fall close to the NGC 2420 sequence when these data are corrected for reddening $E(B-V)_{2158} = 0.43$ (Janes 1979*a*). The locations of the reddening-corrected data are consistent with the idea that the two clusters have similar abundances, $[\text{Fe}/\text{H}] \sim -0.5$ (McClure, Forrester, and Gibson 1974; Janes 1979*a*). At the level of precision of the simulated photometry, differences in age (NGC 2158: 8×10^8 yr, Arp and Cuffey 1962; NGC 2420: 4×10^9 yr, McClure, Newell, and Barnes 1978) are marginally discernible for these two clusters.

In summary, it appears that indices simulated from IIDS spectrophotometry can reliably reproduce photometric values, as tested with DDO data. Based on this feasibility study, it is proposed that stellar parameters for the program stars can be evaluated from simulated indices if reddening effects are accounted for or at least minimized.

The simulated DDO indices for program stars in King 8 and Be 19 are symbolized in Figures 2*c*–2*f* (*circles* and *squares*, respectively). Filled symbols represent observed values. The

open, “dereddened” symbols were derived with the iterative procedure described by Janes (1977) using observed $C(45-48)$, $C(42-45)$, and $B-V$ colors to converge upon $E(B-V)$ and self-consistent intrinsic photometric colors. In principle, the technique should be modified for application to metal-poor stars to account for the significant deblanketing adjustments described by Janes (1979*b*), Osborn (1979), and Hartkopf and Yoss (1983). In practice, it was found that indeterminant reddening and uncertainties in the photometric indices caused the solutions to be nonunique for most program stars. Best estimates for the stellar parameters are presented in Table 3. Although it was not possible to obtain highly accurate values for suspected cluster members, the attempt to identify nearby field stars was successful. These stars are marked “field” in the table. In the following discussion, the reddening values $E(B-V) = 0.55$ and 0.30 were adopted for King 8 and Be 19, respectively. These values are consistent with the broad-band as well as the narrow-band photometry.

b) Supplementary Indices

As anticipated, reddening effects had a significant influence on the interpretation of the photometry, especially the DDO data. Therefore, nearly “reddening-free” indices were devised and examined to characterize the empirical relationships between the program stars and the calibration grid (Table 2 and Table 4). These indices are designed in the spirit of the Q -indices described by Zinn (1980), but do not reproduce Q_{39} , Q_{gr} , or Q_{uv} explicitly due to the limited spectral range observed with the IIDS.

As in similar studies, the indices were constructed after extensive visual examination of the observed spectra. Although visual comparison of the spectrophotometry is useful only for qualitative evaluation of spectral features, the method at least has the advantage that large spectral regions can be evaluated simultaneously. In addition, particularly noisy, weak spectral features tend to be subjectively weighted less than more prominent features. Alternatively, parametric analysis of data, such as factor analysis, has been used to attain the same goal quantitatively, although data sets with nonuniform signal-to-noise must be treated with caution (cf. Christian 1982 and references

TABLE 4
SUPPLEMENTARY PHOTOMETRIC INDICES FOR PROGRAM STARS

Object	H β	(4680)	(4400)	S_{44}	Mn/H β	S_{δ}	S_{Ca}	Fe + MgO	Mg b W_{eq}
King 8:									
7	0.919	3.853	3.467	3.922	0.136	0.57	0.83	5.486	...
33	9.053	0.007	-4.342	4.570	-0.343	0.99	1.52	-1.431	...
35	1.439	-0.213	3.611	4.172	0.156	0.58	1.14	5.699	...
61	8.107	-0.500	-7.175	4.617	-0.291	0.94	1.61	-0.350	...
105	4.893	1.641	-1.317	4.252	-0.058	0.68	1.29	0.902	...
107	1.944	3.623	4.039	3.886	0.147	0.59	1.02	-0.341	5.079
109	3.348	1.869	3.508	3.994	0.047	0.58	1.09	2.860	12.470
119	2.216	3.555	1.700	4.295	0.245	0.55	0.88	-4.176	...
143	1.186	1.852	1.042	3.712	0.166	0.54	0.73	5.053	12.328
Be 19:									
3	1.346	3.889	7.889	3.593	0.280	0.48	0.96	3.088	...
13	2.254	2.141	3.092	3.934	0.118	0.52	0.83	4.358	...
30
33	0.668	5.619	3.577	4.218	0.150	0.52	0.83	1.821	14.671
75	-0.127	4.394	7.708	3.702	0.310	0.42	0.81	0.380	32.390
83	1.603	-0.286	10.095	3.845	0.128	0.58	0.72	2.171	7.703
101	1.049	7.026	4.641	3.935	0.271	0.59	1.00	3.174	11.799
106
116	1.794	1.961	6.141	3.880	0.195	0.53	1.00	3.368	13.529

therein). In this study, noisy data were screened in the following way: a series of "two index" diagrams was examined to estimate the characteristics of the program objects relative to the comparison objects. Then, the results from the individual studies were combined to estimate an average set of parameters for each star. Finally, the abundance estimates for suspected members were averaged to estimate cluster abundances. It is hoped that the *averaged* quantitative values are better estimates of intrinsic stellar parameters than values derived from any single pair of photometric indices.

Consider, for example, Figures 3a and 3b, which exhibit a reddening-free index, $W_{eq}(4680)$, as a function of two indices sensitive to temperature. The index $W_{eq}(4680)$ is the equivalent width measured across the broad blend of atomic lines at $\lambda 4680$ (Fig. 1). The $H\beta$ index (Fig. 3a), measuring the equivalent width of $H\beta$, has been used to study the behavior of late-type spectra (Burstein *et al.* 1982; Rabin 1982), while the new $Mn/H\beta$ index (Fig. 3b) is the ratio of absorption due to the atomic features at $\lambda 4788$ relative to $H\beta$. The pair of figures is useful in that reddening affects the two temperature-sensitive indices in the opposite sense (arrows in Fig. 3), as calculated according to Golay's (1974) procedure. Therefore, self-consistent, dereddened indices might be obtained for each object, especially for stars with luminosity classes III to V and spectral types later than F5. The most dramatic separation in these figures occurs among late-type stars with different abundances, as indicated by the sequences for the calibration clusters. At solar metallicity, there is no significant luminosity separation in the indices calculated for field stars observed with either the IIDS or the IRS. By analogy, it is expected that there is no separation in luminosity class for lower abundance stars, although the libraries of spectra do not sample such objects. It also is seen that a "funnel effect" exists for bluer stars: regardless of luminosity class or abundance, the $\lambda 4860$ feature is very weak for stars earlier than $\sim G2$.

i) King 8

In Figure 3 as in Figure 2, stars King 8-33 and 61 appear to be early-type main-sequence stars, most likely cluster members. This idea was verified further by computing the indices S_δ and S_{Ca} , which have been calibrated by Christian and Smith (1983) specifically to classify early-type spectra. In the (S_δ, S_{Ca}) -plane these two stars appear to be early-type dwarfs ($\leq A5$), consistent with the notion that these objects are near or above the cluster main-sequence turnoff, if $E(B-V)_{K8} = 0.55-0.6$ mag. The objects King 8-105 and 109

have indices similar to solar-neighborhood field stars, consistent with the DDO data.

Most of the other King 8 stars scatter near the NGC 2420+2158 sequence which corresponds to $[Fe/H] = -0.5$; however, King 8-7 and 35 are both peculiar in that their positions in Figures 3a and 3b cannot be reconciled by using reddening adjustments. In fact, reddening corrections, if applied, make the data for these stars more disparate. One explanation for the discrepancy might be that the stars are later than spectral type K0, as very cool field stars tend to scatter widely at small values of $H\beta$ (large $Mn/H\beta$) due to the influence of molecular features in some of the measured passbands. Consideration of other spectral indices as well as visual examination of the spectrophotometry suggests that K8-7 and K8-35 are not very late-type stars, however. A more likely explanation is that these stars have indices influenced by observational error; in the case of K8-35 the signal-to-noise is poorer than for other stars in the program sample. Anomalies of this type were found to be typical throughout the analysis, and so, in the end, more weight was given to the average properties of spectral features of a given star than to individual peculiarities.

ii) Be 19

The stars Be 19-3, 13, 101, and 116 all scatter around the NGC 2420-2158 sequence, between the $[Fe/H] = 0.0$ and -1.0 (M3) sequences. Be 19-3 and Be-75 were suspected to be field dwarfs, based on the DDO photometry and a visual inspection of the IIDS spectra. The position of star Be 19-3 in Figure 3 also is consistent with the star being a metal-poor giant, however. According to Figure 3, star Be 19-75 *could* be an extremely metal-poor G star, but the DDO photometry of the star and the visual appearance of the spectrum (strong Mg feature) suggests that the star actually is later than K0. Its position in these diagrams is not inconsistent with this interpretation. Be 19-33 appears to be either a later type giant or a dwarf, not more metal-poor than NGC 2420. The spectral indices of Be 19-83 are peculiar, analogous to K8-35. These two stars could be as metal-poor as M15, but from the appearance of their spectra this interpretation is doubtful.

iii) Additional Measurements

Based on the analysis above, objects which could be evolved cluster members are King 8 numbers 7, 35?, 107, 119, 143, and Be 19 numbers 13, 30?, 33, 83?, 101, 116. The stars appear to be more metal-poor than solar neighborhood stars, similar to

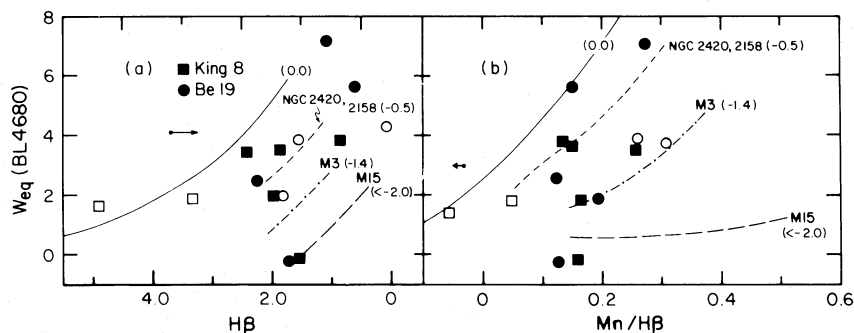


FIG. 3.— $W_{eq}(4680)$ vs. two temperature-sensitive indices. (a) $H\beta$ (Burstein *et al.* 1982) and (b) $Mn/H\beta$ (see text). Arrows indicate the reddening correction for $E(B-V) = 0.5$ mag. The figure suggests that King 8 and Be 19 have metallicities similar to NGC 2420 and NGC 2158, i.e., $[Fe/H] = -0.5$. Open circles represent objects which may be field stars.

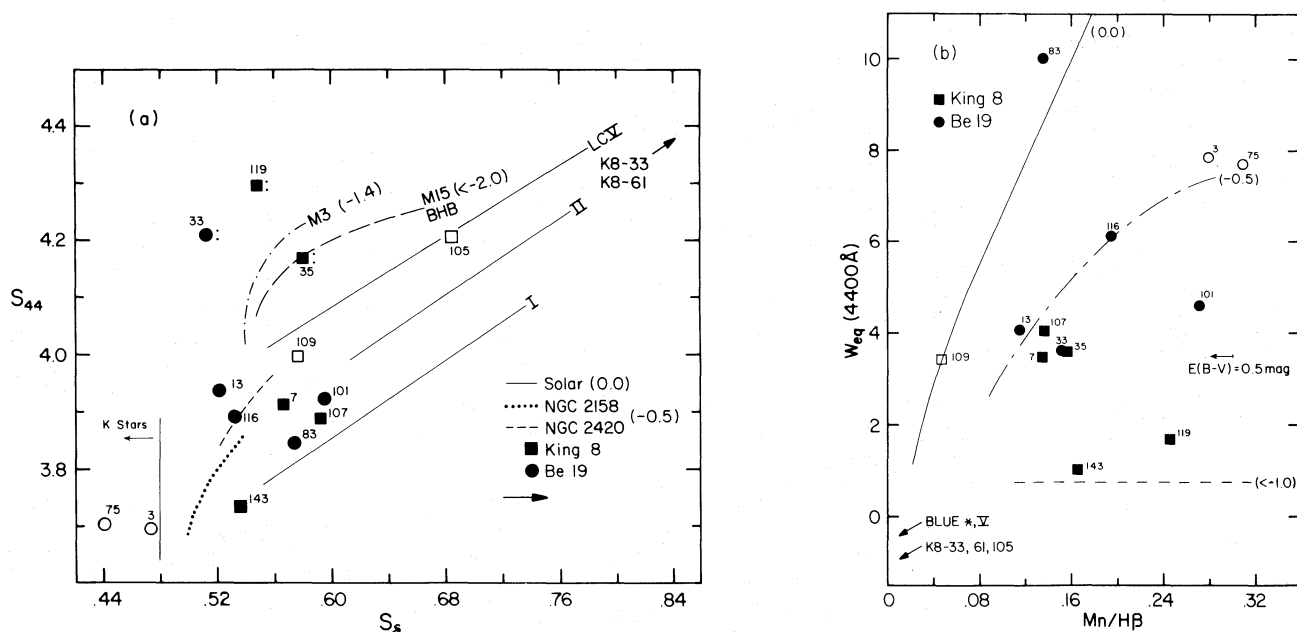


FIG. 4.—(a) The (S_{44}, S_{δ}) -plane (cf. Christian and Smith 1983) for calibration objects and program stars. Luminosity class III sequences are shown with metallicities indicated in parenthesis. Luminosity class V and III sequences are coincident for F and G stars with $[Fe/H] = 0.0$ (solid line). The arrow shows the displacement exhibited by a dereddened point with $E(B-V) = 0.5$ mag. Observed values for King 8 and Be 19 stars are shown as squares and circles, respectively. (b) The $W_{eq}(4400)$ vs. $Mn/H\beta$ indices. Open symbols represent objects which may be field stars.

NGC 2158 and NGC 2420 stars. Few of the stars appear to be more metal-poor than stars in M3. Supporting evidence derives from Figures 4 and 5. In Figures 4a and 4b, two indices which sample atomic line blends near $\lambda 4400$ are shown plotted against temperature sensitive indices S_{δ} and $Mn/H\beta$. Calibration lines in Figure 4a (Christian and Smith 1983) were

extended to later type stars using the expanded grid of stars observed with the IIDS and IRS. The loci of the giant branches for the calibration clusters are labeled and shown as curved sequences; the brightest (tip) stars are at the lowest extreme of the curve (S_{44} small). Thus, the figure resembles an inverted and reflected H-R diagram. Figure 4b exhibits the variation of the equivalent width of a narrower feature at $\lambda 4400$ (Fig. 1 and Table 2). In this figure, solar abundance stars fall near the solid line (marked "0.0") with some considerable scatter, regardless of luminosity class. Stars in NGC 2420 and 2158 are shown by the dot-dashed line, and members of M3 and M15 are indicated by the dashed line. The separation between very metal-poor stars, $[Fe/H] < -1.0$, is much more significant than the separation among higher metallicity stars, and therefore these diagrams can be used to identify extremely metal deficient objects.

Figures 5a and 5b show two indices that change inversely with temperature as a function of $H\beta$. The data for field stars and calibration clusters, as indicated in the figures, show that the most metal-poor stars are clearly distinct from stars with more normal abundance (i.e., $[Fe/H] > -0.8$). Note that in Figure 5b, some objects are absent, including M3 stars, because the $Mg\ b\ W_{eq}$ could not always be calculated due to the red cutoff of the spectral range observed for some data sets.

In general, it is seen that King 8 and Be 19 stars tend to scatter closer to the solar/NGC 2420 data, although some program stars exhibit peculiarities. Figures 4 and 5 support the idea that King 8-109, K8-105, Be 19-3, and Be 19-75 are most likely field stars. The latter two stars have features more characteristic of K stars. The individual peculiarities exhibited by some stars (such as Be 19-35 and K8-143) most likely are due to observational error.

The IIDS data indicate it is unlikely that many of the objects near King 8 or Be 19 stars are extremely metal-poor. In order to estimate the mean properties of each cluster member and, in turn, the average cluster properties, spectral types and abun-

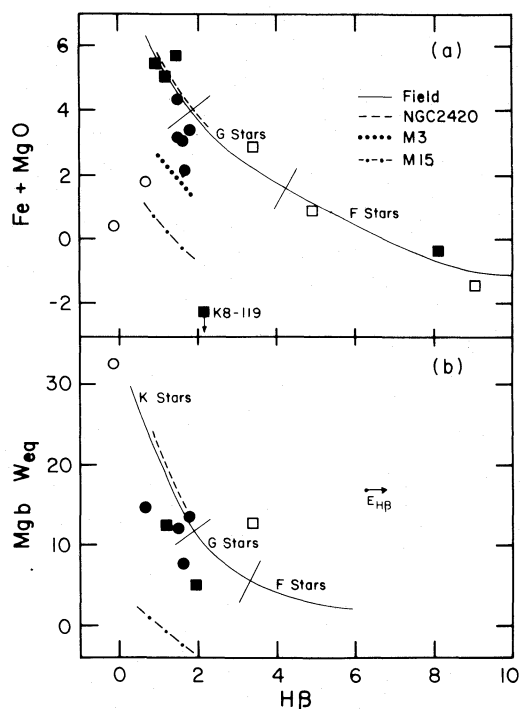


FIG. 5.—Two indices $Fe + MgO$ and $Mg\ b\ W_{eq}$ vs. $H\beta$. These two indices measure absorption features in the red part of the spectrum, a region where most program stars have better signal to noise. Symbols as in Figs. 3 and 4.

dance estimates ("solar," "intermediate," or "metal-poor") from each pair of indices were tabulated for all program stars later than type F0. The estimates were averaged, and are listed in Table 5. The spectral classes represent apparent spectral classes based on line strengths, relative to the classifications of the IRS data and the published DDO sequences. The classifications should be fairly closely related to the spectral classes described by Osborn (1979) based on DDO data because they are derived from spectrophotometry. Therefore, intrinsic $(B - V)$'s were adopted from Osborn's study, to estimate cluster reddenings and check the consistency of the analysis. It can be seen from Table 5 that the adopted reddenings for individual stars are close to the expected cluster reddenings. The average parameters for cluster giants are shown in the last entries of Table 5.

IV. SUMMARY AND DISCUSSION

IIDS spectrophotometric data of stars in the fields of the clusters King 8 and Be 19 have revealed the following information when compared to a grid of comparison stars:

a) DDO indices were successfully simulated from the IIDS spectrophotometry and compared to existing data for clusters and isolated solar neighborhood (low reddening) data. The feasibility study indicated that spectrophotometric indices of this type can be used to estimate intrinsic stellar photometry, and therefore intrinsic stellar parameters. A few field stars were identified with the DDO indices; more highly reddened cluster members were analyzed with a new set of "reddening free" indices.

b) Stars King 8-105, King 8-109, Be 19-3, Be 19-75, and possibly Be 19-83 are field stars, as determined from the simulated photometric indices. The classifications are consistent with a visual examination of the spectra.

c) Stars King 8-33 and 61 appear to be early-type ($\leq A5$) dwarfs reddened by about $E(B - V) = 0.5$ mag. The spectral types are consistent with and serve to verify the photometrically derived age of the cluster (8×10^8 yr; Paper II). The

reddening is slightly less than that found in Paper II, but within the combined errors of the two data sets. The photometric indices of star Be 19-106 are consistent with the idea that this star is a slightly reddened early-type cluster member near the main-sequence turnoff but the signal-to-noise of the spectrum (\sim spectral type A) is so poor as to preclude any more definitive conclusions.

d) The remainder of the stars appear to be evolved cluster members. Although the spectra of these stars have varying degrees of signal-to-noise which complicates the analysis, the mean behavior of simulated photometric indices for these stars suggests that the average metallicities of the two clusters are similar and are analogous to NGC 2420 and NGC 2158 ($[\text{Fe}/\text{H}] = -0.5$). There is little evidence that the clusters could be as metal-rich as solar neighborhood stars, or as metal-poor as the globular cluster M3. Previous studies have suggested that older open clusters may not survive in the solar neighborhood due to dynamical effects, but the evidence for anticenter clusters is that objects older than 5×10^8 yr have survived in spite of their low masses. The three anticenter clusters considered here, King 8, Be 19, and NGC 2158, appear to have ages in the range $0.5\text{--}5 \times 10^9$ yr and similar metallicities, $[\text{Fe}/\text{H}] = -0.3$ to -0.5 . Assuming that the cluster abundances are primordial and the current galactocentric distances of the clusters (11–13 kpc) are representative of the clusters' mean positions in the disk, the galactic abundance gradient 10^9 yr ago was approximately $d[\text{Fe}/\text{H}]/dR \sim -0.8$ dex kpc^{-1} . (The metallicity of the solar neighborhood is taken to be $[\text{Fe}/\text{H}] = 0.0$ to 0.1×10^9 yr ago according to Twarog's 1980 data). This value is in good agreement with the abundance gradient Janes (1979a) derived from K giant stars, which most likely have ages similar to the cluster giants. The abundance gradient exhibited by extremely young objects appears to be the same (cf. the discussion by Christian and Smith 1983). These data suggest that the abundance gradient has not evolved since it was established 10^9 yr ago, and perhaps since the formation of the disk. Therefore, nucleosynthesis, infall,

TABLE 5
STELLAR PROPERTIES AVERAGED FROM SPECTROPHOTOMETRIC INDICES
(Stars later than F0)

Object	Spectral Class	Membership	$\sim [\text{Fe}/\text{H}]^a$	$E(B - V)^b$
King 8:				
7	K0 II–III	yes	–0.4	0.4
35	G8 III	yes	–0.4:	0.4
105	F3 V	no	0.0	0.0
107	G6 III	yes	–0.5	0.5
109	G5 V	no	0.0	0.4?
119	G8 III	yes	–0.5:	0.20:
143	K2 II–III	yes	–0.5	0.4
Be 19:				
3	K2 III–IV	no	–0.1	0.3
13	K0 III	yes	–0.3	0.3
33	G9 III	yes	–0.3	0.2
75	K5 IV–V	no	0.0:	<0.2
83	G6 IV	no?	–0.2	0.4
101	G6 III	yes	–0.3	0.4
116	G6 III	?	–0.5	0.3:
King 8	Analogous to NGC 2420		–0.4	...
Be 19	Slightly metal-poor		–0.3	...

^a Abundances ± 0.2 dex, averaged from individual estimates based on spectrophotometry. A colon indicates values are very uncertain.

^b $(B - V)_0$'s adopted from Osborn 1979 to calculate $E(B - V)$.

and star formation rates seem to be balanced so that no net increase in metallicity occurs at galactocentric distances greater than 8 kpc.

To date, no definitive evidence exists for the existence of *extremely* metal-poor objects in the outer part of the galactic disk. Spurred by the knowledge that some clusters as old as

3×10^9 yr have formed far from the galactic center, it is of interest to determine whether objects with $[\text{Fe}/\text{H}] < -0.8$ ever formed in the outer most reaches of the galactic plane.

The author wishes to thank J. Rose, H. Smith, and J. Heasley for helpful discussions and useful criticisms.

REFERENCES

- Arp, H., and Cuffey, J. 1962, *Ap. J.*, **136**, 51.
 Bell, R. A., and Gustafsson, B. 1978, *Astr. Ap. Suppl.*, **34**, 229.
 Burstein, D., Faber, S., Gaskell, C. M., and Krumm, N. 1982, in *IAU Colloquium 68, Astrophysical Parameters for Globular Clusters*, ed. A. G. D. Philip (Schenectady: L. Davis Press, Inc), p. 441.
 Christian, C. A. 1980, *A.J.*, **85**, 700 (Paper I).
 ———. 1981, *Ap. J.*, **246**, 827 (Paper II).
 ———. 1982, *Ap. J. Suppl.*, **49**, 405.
 Christian, C. A., and Smith, H. A. 1983, *Pub. A.S.P.*, **95**, 169.
 Fay, T., Jr., Stein, W. L., and Warren, W. H., Jr. 1973, in *Proceedings of the Conference on Red Giant Stars*, ed. H. R. Johnson, J. P. Mutschlechner, and B. F. Perry, Jr. (Bloomington: University of Indiana Press).
 Freeman, K. C. 1980, in *Globular Clusters*, ed. D. Hanes and B. Madore (Cambridge: Cambridge University Press), pp. 103 and 361.
 Golay, M. 1974, *Introduction to Astronomical Photometry* (Boston: Reidel).
 Hartkopf, W. I., and Yoss, K. M. 1983, *A.J.*, **87**, 1679.
 Hesser, J. E., Hartwick, F. D. A., and McClure, R. D. 1977, *Ap. J. Suppl.*, **33**, 471 (HHM).
 Jacoby, G., Hunter, D., and Christian, C. 1984, *Ap. J. Suppl.*, **56**, in press.
 Janes, K. A. 1977, *Pub. A.S.P.*, **89**, 576.
 ———. 1979a, *Ap. J. Suppl.*, **39**, 135.
 ———. 1979b, *Dudley Obs. Rept.*, **14**, 103.
 Janes, K. A., and Adler, D. 1982, *Ap. J. Suppl.*, **49**, 425.
 Keenan, P. C., and McNeil, C. 1976, *An Atlas of the Cooler Stars Types G, K, M, S, and C* (Columbus: Ohio State University Press).
 Kraft, R. 1979, *Ann. Rev. Astr. Ap.*, **17**, 309.
 McClure, R. D., Forrester, T., and Gibson, J. 1974, *Ap. J.*, **189**, 409.
 McClure, R. D., Newell, B., and Barnes, J. 1978, *Pub. A.S.P.*, **90**, 170.
 McClure, R. D., and van den Berg, S. 1968, *A.J.*, **73**, 313.
 Morgan, W. W., Keenan, P. C., and Kellman, E. 1942, *An Atlas of Stellar Spectra* (Chicago: University of Chicago Press).
 Osborn, W. 1979, *Dudley Obs. Rept.*, **14**, 115.
 Rabin, D. 1982, *Ap. J.*, **261**, 85.
 Roman, N. G. 1973, in *IAU Symposium 50, Spectral Classification and Multicolor Photometry*, ed. C. Fehrenbach and B. F. Westerlund (Dordrecht: Reidel), p. 36.
 Sandage, A. 1970, *Ap. J.*, **162**, 841.
 Smith, H. A., and Hesser, J. E. 1983, *Pub. A.S.P.*, **95**, 277.
 Spinrad, H., and Taylor, B. 1969, *Ap. J.*, **157**, 1279.
 Strom, K. 1977, *Standard Stars for IIDS Observations* (Tucson: Kitt Peak).
 Suntzeff, N. B. 1980, *A.J.*, **85**, 408.
 Trefzger, C. F., Carbon, D. F., Langer, G. E., Suntzeff, N. B., and Kraft, R. D. 1983, *Ap. J.*, **266**, 144.
 Twarog, B. A. 1980, *Ap. J.*, **242**, 242.
 van den Bergh, S., and Pritchett, C. 1977, *Ap. J. Suppl.*, **34**, 101.
 Zinn, R. 1980, *Ap. J. Suppl.*, **42**, 19.
 ———. 1983, in *IAU Colloquium 68, Astrophysical Parameters for Globular Clusters*, ed. A. G. Davis Philip and D. S. Hayes (Schenectady: L. Davis Press), p. 45.

CAROL A. CHRISTIAN: Canada-France-Hawaii Telescope Corporation, P.O. Box 1597, Kamuela, HI 96743-1597